Experiments of Pool Boiling Performance (Boiling Heat Transfer and Critical Heat Flux) on Designed Micro-Structures

Seol Ha Kim[a], Jun Young Kang[a], Gi Chol Lee[b], Moriyama Kiyofumi[a], and Moo Hwan Kim[a,c] and Hyun Sun Park[a,*]
[a]*Division of Advanced Nuclear Engineering, POSTECH, Pohang, 790-784, Republic of Korea*
[b]*Department of Mechanical Engineering, POSTECH, Pohang, 790-784, Republic of Korea*
[c]*Korea Institute of Nuclear Safety (KINS), Daejeon, Republic of Korea*
[*]*Corresponding author: hejsunny@postech.ac.kr*

1. Introduction

As one of a key phenomenon in nuclear reactor thermal hydraulics, nucleate boiling has been widely studied by numerous researchers to improve the nuclear plant design efficiency and safety. In general, the evaluation of the boiling performance mainly focuses on two physical parameters: boiling heat transfer (BHT) and critical heat flux (CHF). In the nuclear power plants, both BHT and CHF contribute the nuclear system efficiency and safety, respectively. In this study, BHT and CHF of the pool boiling on well-organized fabricated structured (micro scaled) surface has been evaluated. As a results, BHT change on microstructured surface shows strongly dependent on Pin-fin effect analysis. In terms of CHF, critical size of micro structure for CHF enhancement has been observed and analyzed based on the capillary wicking effect.

2. Methods and Results

A set of experiments was designed to prepare 13 samples; the 12 samples of microstructured surfaces and one bare surface has been fabricated by MEMS (Micro Electro Mechanical Systems) techniques. The samples was tested for the pool boiling experiments at saturated and atmospheric pressure conditions.

2.1 Heating Surface Preparation

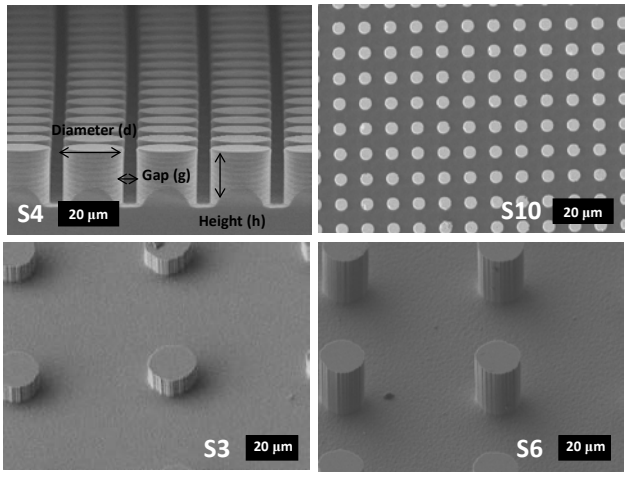

Figure 1. SEM image of prepared micro structures

Table I: Geometric Information of micro structures

Sample No.	d	h	g	r (roughness)
S0	-	-	-	1
S01	20	10	5	2.00
S02	20	10	20	1.39
S03	20	10	40	1.17
S04	20	20	5	3.01
S05	20	20	20	1.79
S06	20	20	40	1.35
S07	20	40	5	5.02
S08	20	40	20	2.57
S09	20	40	40	1.70
S10	5	20	5	4.14
S11	5	20	10	2.40
S12	5	20	20	1.50

Figure 1 shows scanning electron microscopy (SEM) images of representative microstructures used in this study. Table 1 lists the geometric features of the prepared samples (nine structured cases and one bare case). The circular-micro pillar arrays were etched in silicon using deep reactive ion etching (DRIE), with a roughness r, defined as the ratio of the actual area in contact with the liquid to the projected area; the roughness ranged from 1.00 to 4.4. Several length scales (5~40 μm) were designed as geometric parameters (i.e., height, diameter, and gap).

2.2 Experimental Setup

In this study, a pool boiling experiments was carried out as shown Figure 2. The facility was composed of a test sample jig, a main test pool and a lid with an immersion heater (pre-heater) and condenser. The pre-heater applies heat to D.I. water pool for two hours before main experiments. During the two hours, dissolved gas in the water pool would be degassed and saturated condition would be maintained, and the condenser keep a water level by tap water cooling. The test sample jig consisted of a PEEK (polyetheretherketone) test sample frame and silicon test sample. PEEK is a thermoplastic that has high thermal resistance and is compatible with an aqueous environment. The test samples were fixed with adhesive binary epoxy (DuralcoTM 4365). The test sample was heated electrically using a platinum (Pt) electrode, which was deposited on the bottom surface of the silicon wafer.

(Fig. 2) Electrical power was supplied using a Sorensen DLM 300-13E power supply. A data acquisition system (Agilent 34970A) was used to measure the input power (heat flux) and a temperature of the Pt electrode.

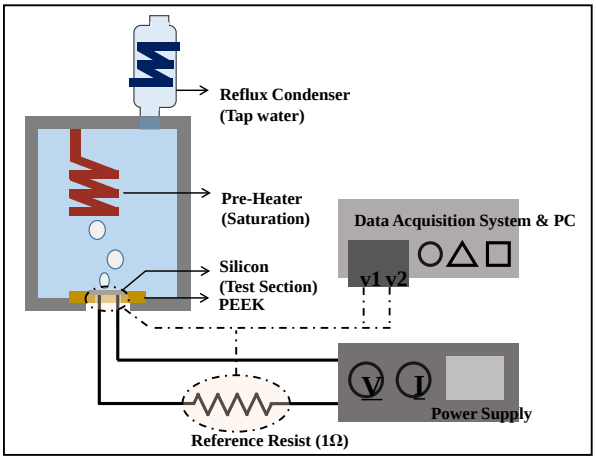

Figure 2. Pool Boiling Experimental Setup

2.3 Results

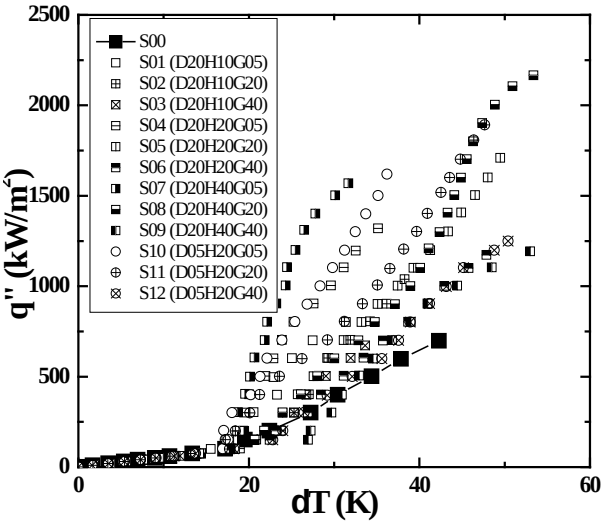

Figure 3. Pool Boiling Performance (Boiling Curve)

Figure 3 shows the boiling experimental results on the smooth Si surface (S0) and microstructured surfaces (S1–S12). The performance plot of the heat flux q" as a function of the wall super heat ΔT=Tw-Tsat, where Tw is the heated surface temperature and Tsat is the saturation temperature, is shown for all cases; the data in Fig. 3 represent the average obtained from two to three rounds of experimental testing (four times for the smooth surface case, S0). The maximum uncertainties in the heat flux and temperature measurements were approximately 6.3% and 2.8 K, respectively. In general, the boiling curves indicated that the structured surfaces (S1–S12) experienced significantly enhanced boiling heat transfer (as evidenced by the slope of the boiling curve) and CHF (heat flux at the end point), compared with the smooth surface (S0). At low super heat regime (before the onset of nucleate boiling, ONB), the boiling heat transfer of the prepared surfaces has no difference. However, after ONB, the boiling heat transfer on structured surface becomes much higher performance compared to the bare surface. Although there are several delayed ONB point on the structured surface, BHT at fully developed nucleate boiling regime (~30K) or near CHF on the structured surface shows higher that on the Bare surface. Its trends along the structured surface would be discussed later chapters. In terms of CHF, the bare smooth surface (S0) exhibited a heat flux of 697.8 ± 44.1 kW m−2 at 42.3 ± 2.8 K, and the S08 case achieved the highest CHF performance with 2165 kW m−2 at 53.39 K (3100% that of the S0 case). Note that S07 had the highest surface roughness; its CHF performance was 1569 kW m−2 at 31.67 K, which was less than both S08 and S09 (both with smaller surface roughness than S07). Additionally, the wall superheat points in S1 were also lower than the other two cases. These experimental results differ from those presented in a previous study that reported a CHF increase with the surface roughness. (Chu et al., 2012)

2.4 BHT Analysis

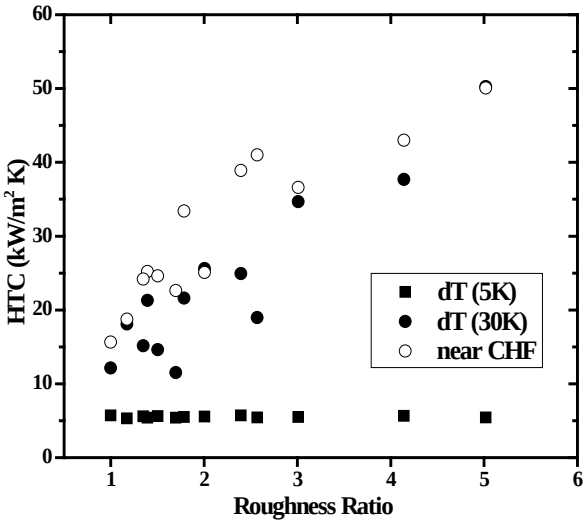

Figure 4. Boiling Heat Transfer Trend (Roughness)

Figure 4 shows the boiling heat transfer trend on structured surface along the roughness ratio. According to the Fig. 4 (a), the Heat Transfer Coefficient (HTC) shows dependency on the roughness factor at high super heat regime and CHF. However, the low super heat regime (before ONB) shows no dependency on samples roughness. Since there no bubble generation before the ONB, only natural convection dominate the heat transfer rate. And, the thermal boundary layer (~100um) of the natural convection regime is higher than the structures height (10~40um) on the heating surface, so the structure couldn't affect the heat transfer rate. However, after ONB, the nucleated bubble behaviors strengthen convective effect, and it affect the thermal boundary layer. Due to the enhanced convective effect on the heating surface by bubble dynamics, the higher heat transfer rate can be obtained from the structured surface with roughness ratio.

2.5 CHF analysis

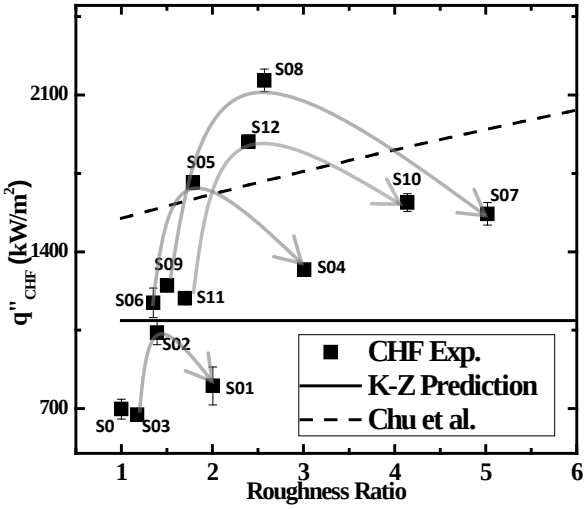

Figure 5. Critical Heat Flux Trend (Roughness)

In Fig. 4(b), solid and dashed lines indicate the CHF prediction from the hydrodynamic instability analysis (Kutateladze–Zuber analysis) [1, 2] and the roughness-capillary effect analysis (Chu et al., 2012) [3], respectively. Because the hydrodynamic instability analysis does not reflect the surface conditions (e.g., wetting and roughness), its prediction is independent of the change in roughness. On the contrary, the roughness-capillary effect analysis and present experimental CHF data generally show an increasing trend with increase in roughness. However, from our data, the S01, S04, S07 and S10 cases with higher roughness values exhibited lower CHF values than S02, S05, S8 and S11 with lower roughness values, respectively. Among those, Samples S01–S03 had the same diameter (20 μm); however, the gap spacing ranged from 5 μm (for S01) to 40 μm (for S03). As the gap between the micropillars decreased (i.e., the roughness increased), the CHF value increased from S03 to S02, but decreased from S02 to S01. This CHF oscillatory tendency (i.e., ups and downs with roughness or changes in the gap) was also observed for Samples S04–S06, S07-S09 and S10-S12; these three samples had the same diameter (20 μm) and different gaps (ranging from 5– 40 μm); here, the CHF also showed an oscillatory trend with changes in the gap. In principle, as the spacing between the micropillars decreases, the roughness factor increases due to an enlarged wetted surface area. Furthermore, the enhanced roughness increased the capillary force of the liquid rewetting the dry bubble patch, resulting in a CHF delay. However, the above experimental results imply that the capillary effects amplified by surface roughness should be limited by a certain critical size of the gap (spacing). Here, we suggest that the liquid in-flow performance, which is directly related to the rewetting capability of the dry patch, decreases with changes in the gap size, due to the reduced permeability of the microstructured surface.

3. Conclusions

In this study, BHT and CHF of the pool boiling on well-organized fabricated structured (micro scaled) surface has been evaluated. As a results, BHT change on microstructured surface shows strongly dependent on the roughness ratio. The extended heat transfer area contributes the boiling heat transfer increase on the structured surface, and its quantitative analysis has been performed. In terms of CHF, the critical size of micro structure for CHF enhancement has been observed and analyzed based on the capillary wicking effect. We suggested a capillary limit to CHF delay for modeling capillary induced liquid inflow through microstructured surfaces. The critical size of the capillary limit on the prepared structured surface, determined by a model, could be reasonable explanation points for the experimental results (optimal size for CHF delay). The present experimental results also showed clearly the critical size (10 ~ 20μm) for CHF delay, predicted by capillary limit analysis. This study provides fundamental insight into BHT and CHF enhancement of structured surfaces, and an optimal design guide for the required CHF and boiling heat-transfer performance. Finally, this study can contribute the basic understanding of the boiling on designed microstructure surface, and it also suggest the optimal micro scaled structured surface of boiling performance. Additionally, the study contributes to new surface technologies with high heat-removal capabilities for not only nuclear thermal hydraulics but also other advanced thermal management applications.

ACKNOLEDGEMENT

This work was supported by National Research Foundation of Korea (NRF) grants funded by the Korean government (MSIP) (2014M2B2A9031122).

REFERENCES

[1] N. Zuber, “Hydrodynamic Aspect of Boiling Heat Transfer,” AEC Report No. AECU-4439 (1968)
[2] S. S. Kutateladze, “On the Transition to Film Boiling under Natural Convection,” Kotloturbostroenie 3, 10–12 (1948)
[3] K. H. Chu, R. Enright, and E. N. Wang, “Structured surfaces for Enhanced Pool Boiling Heat Transfer,” Appl. Phys. Lett. 100(24), 241603 (2012)